GEOPHYSICAL RESEARCH LETTERS, VOL. 27, NO. 15, PAGES 2265-2268, AUGUST 1, 2000

Modeling Climate Shift of El Nino Variability in the Holocene

Zhengyu Liu, J. Kutzbach, Lixin Wu

University of Wisconsin-Madison, Wisconsin

Abstract. A coupled ocean-atmosphere general circulation model is used to investigate climatic shift of El Nino in the Holocene. The model simulates a reduced ENSO intensity in the early and mid- Holocene, in agreement with paleoclimate record. The ENSO reduction is proposed to be caused by both an intensified Asian summer monsoon and a warm water subduction from the South Pacific into the equatorial thermocline.

1. Introduction

El Nino and the Southern Oscillation (ENSO) is a dramatic example of global climate variability that exists not only in the present (Philander, 1990), but also in the past (Rodbell et al., 1999; Hughen et al., 1999). The intensity of ENSO, however, seems to have undergone significant climatic shifts in the Holocene. The analysis of a high resolution 15,000 year record of lake deposits in Ecuador suggests that strong ENSO events became established only about 5000 years ago (Rodbell et al., 1999). Coupled atmosphere-ocean models are beginning to explore Holocene climate (Hewitt and Mitchell, 1998; Otto-Bliesner, 1999; Bush, 1999; Liu et al., 1999). Here, a coupled ocean-atmosphere model is used to investigate Holocene climate and ENSO. Our model simulates a change of the base climate state and reduced ENSO intensity in the early and mid-Holocene, in apparent agreement with the Ecuadorian record. The changed climate and weaker ENSO are proposed to be caused by two mechanisms. First, the higher boreal summer insolation intensifies the Asian summer monsoon, which strengthens the Pacific trades and lowers equatorial ocean temperatures, therefore suppressing warm El Nino events. Second, the stronger austral winter insolation warms the South Pacific surface water, which is then subducted equatorward to weaken the mean equatorial thermocline, also contributing to a reduced ENSO.

2. Model and Experiments

We use a fully coupled ocean-atmosphere model – the Fast Ocean-Atmosphere Model (FOAM) (Jacob R., 1997), in which an atmosphere of resolution R15 is coupled with an ocean of resolution 1.4°×2.8°. The model physics are similar to those of the NCAR CSM (Meehl and Arblaster, 1998). A modern control is run for 600 years without flux correction, in which FOAM reproduces most major features of the present climate in the tropics, as does the NCAR CSM. In particular, tropical climate variability is dominated by an ENSO mode, with the maximum SST variability in the eastern equatorial Pacific (Fig.1), and with the power spectrum peaked in periods of 2 -7 years (Fig.2). As in observations (Rasmusson and Carpenter, 1982), both the warm El Nino and cold La Nina events tend to be phase-locked with the seasonal cycle, with eastern Pacific SST anomalies peaking in boreal winter.

Climate variability of the early and mid Holocene is simulated in two experiments for 6ka and 11ka, which are forced by the insolation of 6ka and 11ka, respectively (Berger, 1978). These Holocene simulations start from the 450th year of the modern run. They are then integrated for 150 years with the last 120 years used for comparison with the modern run of the same years. These experiments test only the sensitivity of climate to orbital changes, because Holocene changes in atmospheric CO_2 concentration and in residual late glacial ice sheets are not included as prescribed boundary conditions. One striking feature of the 6ka and 11ka simulations is a substantial reduction of ENSO variability (Fig.2). The reduction of variance in the periods of 2-7 years is over 20% (Table 1).

3. Mechanisms

The reduced ENSO intensity in the 6ka and 11ka simulations appears to be caused by changes in the base state climate that are attributable to two mechanisms. One mechanism is the enhancement of the South Asian summer monsoon, which occurs due to changes in earth's orbit (Kutzbach and Otto-Bleisner, 1982). During the early to mid-Holocene, the earth is the closest to the sun from June to September, and, therefore, the northern hemisphere solar radiation is enhanced in boreal summer relative to the present. This increase of summer insolation enhances the Asian summer monsoon significantly. The intensified deep convection in the Asian monsoon region increases the Pacific easterly trades through the atmospheric Walker Circulation, which then forces a stronger upwelling cooling in the central-eastern equatorial Pacific (Barnett et al., 1989). The colder eastern Pacific SST further strengthens the trades through the Bjerknes (1969) feedback mechanism. The combination of Asian monsoon forcing and positive ocean-atmosphere feedback finally leads to

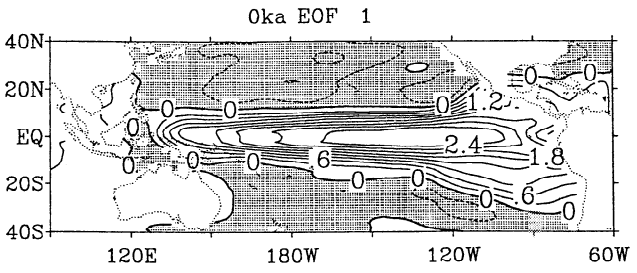

Figure 1: The pattern of 1st EOF of SST for the modern run, which shows the spatial pattern of the El Nino mode (contour interval arbitrary). The time series of the EOF coefficient (not shown) resembles closely the time series of SST in eastern equatorial Pacific region.

Paper number 2000GL011452.
0094-8276/00/2000GL011452$05.00

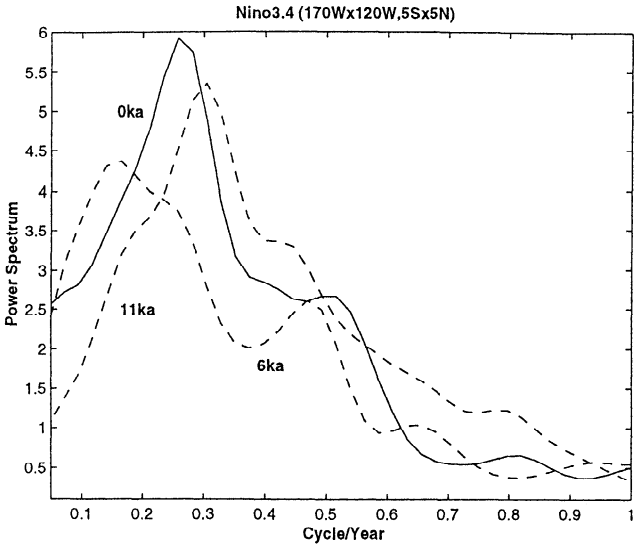

Figure 2: The variance spectrum (units arbitrary) of eastern equatorial Pacific SST (Nino 3.4, 170°W--120°W, 5°S--5°N) for the modern run (solid) and 6ka and 11ka runs (dashes).

Table 1. Measures of Nino 3.4 (170°W-120°W, 5°S-5°N) SST anomaly behavior for modern, 6ka and 11ka simulations: variance in ENSO band (2-7 year), and amplitude of El Nino and La Nina (SST anomaly averaged for the 10 strongest events). The variance is calculated from the power spectrum in Fig.2 integrated over the 2 – 7 years band. The amplitude of El Nino and La Nina events are calculated with respect to the seasonal climatology of each run.

	Moder	*6ka*	*11ka*
Variance (ENSO band)	0.15	0.12	0.13
El Nino SST anomaly (°C)	1.05	0.93	0.93
La Nina SST anomaly (°C)	-0.85	-0.88	-0.90

a trade wind increase of about 20% (Fig.3a) and a SST cooling of over 0.5°C (Fig.3b) over the central/eastern Pacific. Since ENSO grows the most rapidly in early summer (Zebiak and Cane, 1987; Webster and Yang, 1992), this enhancement of upwelling cooling due to the stronger monsoon can efficiently suppress the initial growth of a warm El Nino event in summer and then reduce its peak amplitude later in the year (Barnett et al., 1989). By the same argument, interestingly, cold La Nina

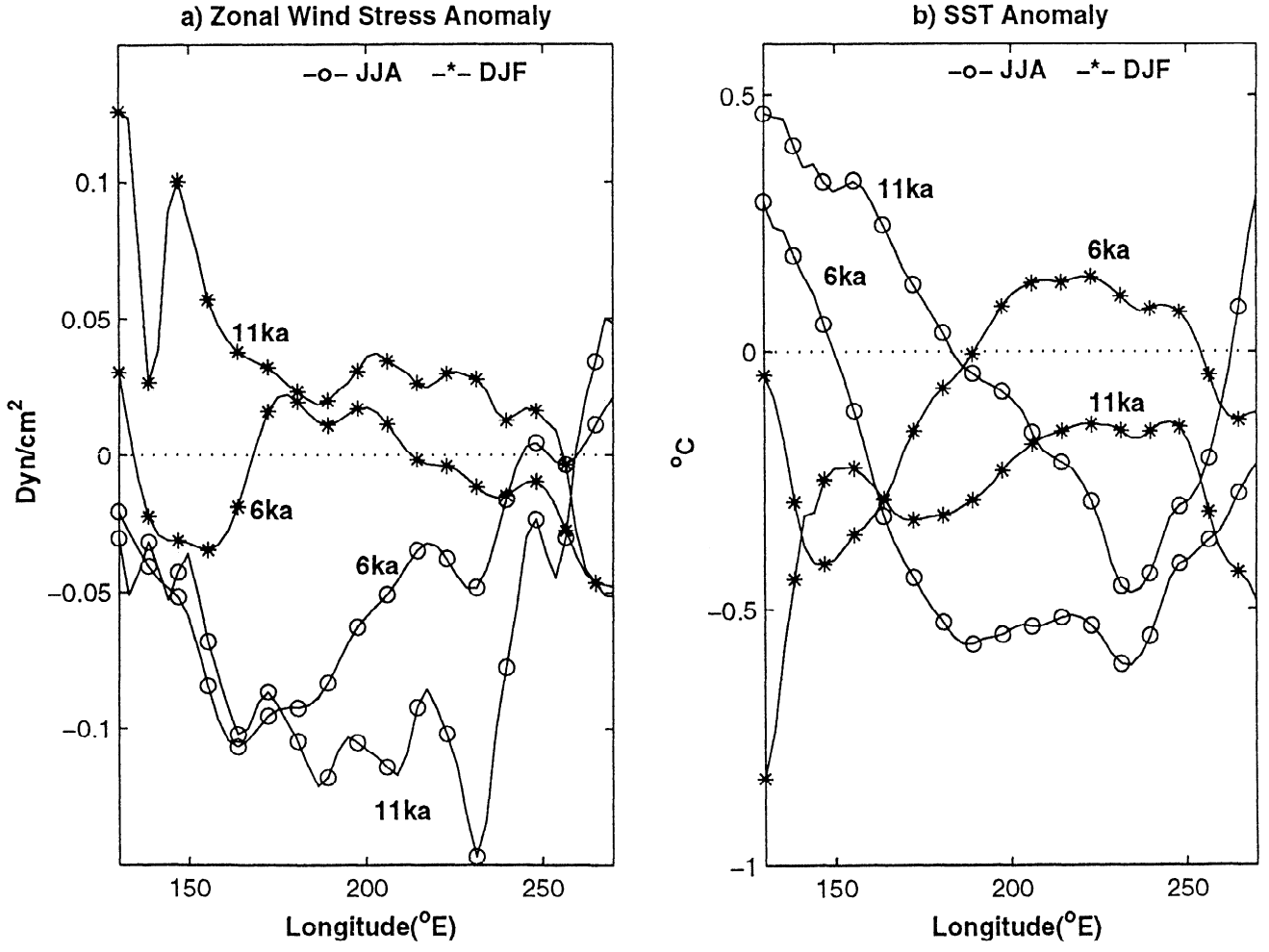

Figure 3: The changes (6ka and 11ka minus modern) of (a) zonal wind stress and (b) SST averaged within 5° of the equator in the Pacific sector. The JJA (June, July, August) and DJF (December, January, February) averages are plotted in open circles and stars, respectively.

events should be intensified. This is indeed the tendency in our model. As shown in Table 1, the largest Holocene SST anomalies are reduced by over 10% for warm El Nino events, but are enhanced slightly (less than 5%) for cold La Nina events. The amplitude reduction of warm El Nino events is larger than the modest amplitude increase of cold La Nina events, resulting in a reduction of total variance of interannual variability at 6ka and 11ka (Fig.2, Table 1).

Additional evidences from the model behavior also seem to support the linkage between Asian monsoon and ENSO. The correlation between the interannual variability of the eastern equatorial Pacific SST and Asian monsoon precipitation (averaged for 60°E-120°E, 10°N-30°N) is negative in the simulations, as in present day observations (Shukla, 1987). The maximum lagged cross-correlation peaks at –0.28, –0.35 and –0.45 in the modern, 6ka and 11ka simulations, respectively. This result implies a stronger connection between ENSO and Asian monsoon precipitation in the 6ka and 11ka simulations than in the modern control. Furthermore, the simulated maximum ENSO variability seems to be shifted towards the western equatorial Pacific at 6ka and 11ka (not shown). Indeed, the variance of interannual SST variability west of the dateline increases from 0.06 in the modern run, to 0.09 and 0.084 in the 6ka and 11ka runs, respectively, opposite to the situation in the central/eastern Pacific. The westward shift could be an indication of a stronger interaction between ENSO and the South Asian monsoon, because the Asian monsoon influences the western Pacific winds most directly. In addition, our recent theoretical work (Liu, 2000) suggests that an enhanced seasonal monsoon wind should reduce the amplitude of ENSO because of the nonlinear mechanism of frequency entrainment.

The other mechanism that may contribute to the reduced early to mid-Holocene ENSO is the weakening of the background equatorial thermocline below about 50 to 100 meters. The eastern equatorial Pacific thermocline temperature is increased by about 0.2°C in both the 6ka and 11ka simulations (Fig.4a,b). This warm subsurface temperature anomaly deepens and weakens the background equatorial thermocline, which, in turn, could reduce the ability of the upwelling water to affect SST, and therefore suppress ENSO variability (Zebiak and Cane, 1987). A similar argument has been used to explain the sensitivity of ENSO to CO_2 increase (Timmermann et al., 1999). In our simulations, the warm subsurface equatorial water can be traced back to the South Pacific subtropical ocean, as seen in Fig.4, and can be explained by the change of insolation. In the early to mid-Holocene, the increase of solar radiation in boreal summer (or austral winter), while intensifying the Asian monsoon in the northern hemisphere, warms the austral winter surface water in the South Pacific Ocean (up to 0.5°C – 1°C). This surface water, warmer at 6ka and 11ka than in the control, is mixed down to the subsurface oceanic thermocline due to later winter convection, where it is eventually ventilated into the equatorial thermocline (Liu et al., 1994). In the North Pacific, the decreased winter insolation leads to downward mixing of colder surface water at 6ka and 11ka. In the equatorial region, the warm water subducted from the South Pacific overwhelms the cold water from the North Pacific (Fig.4a,b). The weaker equatorward ventilation from the North Pacific is likely to be caused by the blocking effect of the North Equatorial Counter Current (Lu and McCreary, 1995) and the leaking of North Pacific water to the Indian Ocean via Indonesian Throughflow (Rodgers et al., 1999).

4. Discussions

The reduced ENSO intensity in our 6ka and 11ka experiments appears to be consistent with the paleoclimate record from Ecuador (Rodbell et al., 1999) and perhaps elsewhere. However, the observational record is far from adequate, and, model simulations still have many questions (see below); therefore detailed data/model comparison seems premature. Shells found in archaeological deposits in northern Peru (Sandweiss et al., 1996) have been interpreted as the evidence of a permanent warm eastern equatorial Pacific prior to the mid-Holocene. Our early and mid- Holocene simulations, however, produce an annual mean SST colder than today over most of the open eastern equatorial Pacific, as do other simulations (Otto-Bliesner, 1999; Bush, 1999; Clement et al., 1999). Nevertheless, in a band of about 1000 km along the South America coast from the subtropics to the equator, the annual mean SST in our model is slightly warmer than present at both 6ka and 11ka (not shown). This coastal warming seems to be caused by the reduced along-shore wind associated of the South Pacific subtropical high. In spite of model deficiencies in the region of South America coast (poor representation of Andes in the atmosphere and poor horizontal resolution in the ocean), it is possible that the Peruvian evidence (Sandweiss et al., 1996) could instead be consistent with our result if interpreted more conservatively as a regional coastal oceanic condition, rather than an indicator for the entire central-eastern equatorial Pacific. Finally, in contrast to the colder central/eastern equatorial Pacific, the annual mean SST is slightly higher west of about 160°E in our 6ka and 11ka

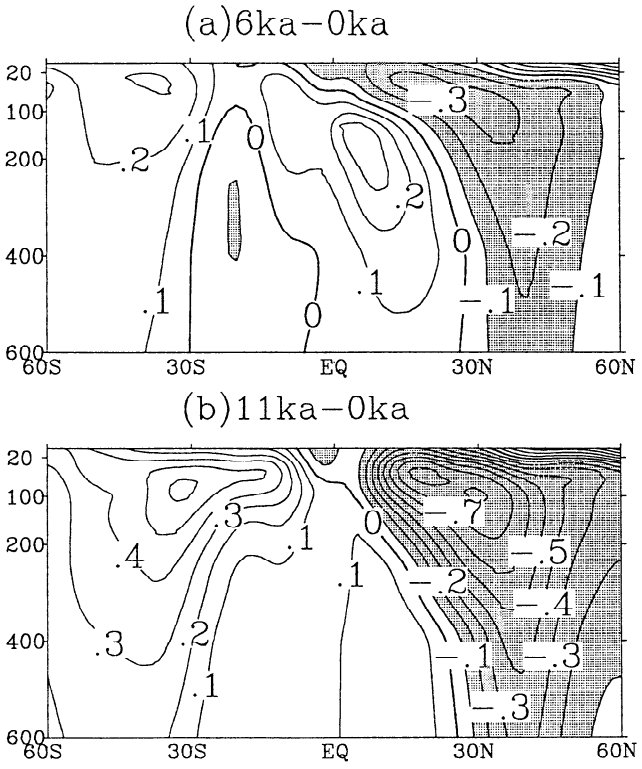

Figure 4: Differences of annual mean ocean temperatures between (a) the 6ka run and the modern run, and (b) the 11ka run and the modern run, zonally averaged in the eastern Pacific (180°W-100°W). Contour interval is 0.1°C. Regions less than –0.1°C are shaded.

simulations, compared to the control (not shown). This warmer western Pacific, which extends from about 10°N to 30°S, seems to agree in sign with coral-based maximum temperature estimates for 6ka from the Great Barrier Reef (Gagan et al., 1998). Other 6ka simulations, however, do not show this warming feature (Otto-Bliesner, 1999; Bush, 1999).

The major features in the FOAM simulations seem to be robust and were reproduced in another set of experiments in a preliminary study (Liu et al., 1999). Nevertheless, some of our conclusions may be affected by deficiencies of the model. The model El Nino is about 40% weaker in the modern run than in present observations, and the reduction of ENSO intensity in our 6ka and 11ka simulations also seems to be less than the reduction that is implied by proxy records (Rodbell et al., 1999). This disagreement could be related to the models' thermocline being too diffusive. A sharper equatorial thermocline could make the upwelling more effective and therefore increase the strength and sensitivity of El Nino (Meehl et al., 2000). The oceanic subduction process from the South Pacific may also be underestimated in our model. This is because FOAM tends to produce a double ITCZ, as in many coupled models (Mechoso et al., 1995). Therefore, the model climatology is too symmetric about the equator. In reality, the ITCZ occurs predominantly north of the equator, which can block the subduction from the North Pacific more effectively (Lu and McCreary, 1995). Thus, the subduction mechanism may be more important in reality than is demonstrated in FOAM. Finally, the phase locking of our model ENSO tends to shift systematically: the peak SST anomaly shifts from December in the control towards the next June at 6ka and especially 11ka. This result could be related to FOAM's deficient simulation of equatorial annual cycle in the eastern Pacific Ocean.

Clement et al. (1999, 2000) have recent proposed a mechanism for the suppression of ENSO before the mid-Holocene. Their mechanism involves ocean/atmosphere processes locally within the equatorial Pacific region, which is initiated by the anomalous insolation forcing from later summer to early fall in the eastern equatorial Pacific. The possibility of multiple mechanisms suggests that the cause for the climatic shift of ENSO in the Holocene may be complex. Improved models and observations are needed to better understand the evolution of ENSO in the past as well as in the present and future.

Acknowledgement. We thank Dr. R. Jacob for performing FOAM experiments in a preliminary study (Liu et al., 1999) and for helping us to perform the FOAM experiments in this study. Discussions with Drs. M. Cane, G. Meehl, G. Philander and B. Wang are greatly appreciated. P. Behling and R. Selin have helped the processing of FOAM data. This work is supported by NSF. A computer time grant from the DoD HPCMO is greatly appreciated.

References

Barnett, T.P., et al., The effect of Eurasian snow cover on regional and global climate variations. *J. Atmos. Sci.*, **48**, 661-685 (1989).

Berger, A.L., Long-term variations of caloric insolation resulting from the earth's orbital elements. *Quat. Res.*, **9**, 139-167 (1978)

Bjerknes, J. Atmospheric teleconnection from equatorial Pacific. *Mon. Wea. Rev.*, **97**, 163-172 (1969).

Bush, A. Assessing the impact of Mid-Holocene insolation on the atmosphere-ocean system. *Geophys. Res. Lett.*, **26**, 99-102 (1999).

Clement, A.C., Seager, R. and Cane, M.A. Orbital controls on ENSO and tropical climate. *Paleoceanography*, **14**, 441-456 (1999).

Clement, A.C., Seager, R. and Cane, M. A., Suppression of El Nino during the mid-Holocene by changes in the Earth's orbit. *Paleoceanography*, in press (2000).

Gagan M. K. et al., Temperature and surface – ocean water balance of the mid-Holocene tropical western Pacific. *Science*, 279, 1014-1018 (1998).

Hewitt, C.D and Mitchell J.F.B., A fully coupled GCM simulation of the climate of the mid-Holcene. *Geophys. Res. Lett.*, **25**, 361-394 (1998)

Hughen K. et al., El Nino during the last interglacial period recorded by a fossil coral from Indonesia. *Geophys. Res. Lett.*, **26**, 3129-3132 (1999)

Jacob R. Low frequency variability in a simulated atmosphere ocean system. *Ph.D thesis, University of Wisconsin – Madison* (1997)

Kutzbach J.E. and Otto-Bleisner, B. L. The sensitivity of the African-Asian monsoonal climate to orbital parameter changes for 9000 years in a low resolution general circulation model. *J. Atmos. Sci.*, **39**, 1177-1188 (1982).

Liu, Z. et al. Monsoon impact on El Nino variability in the early Holocene. *PAGES Newsletter*, Vol. 7, No.2, 16-17 (1999).

Liu, Z., Philander, S.G.H. and Pacanowski R. C. A GCM study of tropical -subtropical upper ocean mass exchange. *J. Phys. Oceanogr.*, **24**, 2606-2623 (1994).

Liu, Z., A theory of monsoon influence on ENSO. *J. Clim.*, to be submitted.

Lu, P. and McCreary, J. P. Influence of the ITCZ on the flow of the thermocline water from the subtropical to the equatorial Pacific Ocean. *J. Phys. Oceanogr.*, **25**, 3076-3088 (1995).

Mechoso, C. R. et al. The seasonal cycle over the tropical Pacific in coupled ocean-atmosphere general circulation models. *Mon. Wea. Rev.*, **123**, 2825-2838 (1995).

Meehl G. A. and Arblaster, J. M. The Asian-Australian monsoon and El Nino-Southern Oscillation in the NCAR Climate System Model. *J. Climate*, **11**, 1356-1385 (1998)

Meehl G. A. et al. Anthropogenic forcing and decadal climate variability in sensitivity experiments of 20th and 21st century climate. *J. Clim.*, in press (2000).

Otto-Bliesner B.L., El Nino/La Nina and Sahel precipitation during the middle Holocene. *Geophys. Res., Lett.*, **26**, 87-90 (1999)

Philander, S. G. H. El Nino, La Nina, and the Southern Oscillation. (Academic Press, San Diego, 1990)

Rasmusson, E.M. and Carpenter, T.H. Variations in tropical sea surface temperature and surface wind fields associated with the Southern/Oscillation/El Nino. *Mon. Wea. Rev.*, **110**, 354-384 (1982).

Rodbell, D. T et al., An ~15,000-year record of El Nino – Driven Alluviation in southwestern Ecuador *Science*, **283**, 516-520 (1999).

Rodgers, K. et al. The role of Indonesian Throughflow in equatorial Pacific thermocline ventilation. *J. Geophys. Res.*, 104, 20,551-20570 (1999).

Sandweiss D. et al, Geoarchaeological evidence from Peru for a 5000 years B.P. onset of El Nino, *Science*, **273**, 1531-1533 (1996).

Shukla J. Interannual variability of monsoons. In *Monsoons*, edited by J.S. Fein and P.L. Stephens, 399-464, John Wiley and sons (1987).

Timmermann, A. et al. Increased El Nino frequency in a climate model forced by future greenhouse warming. *Nature*, **398**, 694-697 (1999).

Webster P. and Yang, S. Monsoon and ENSO: selectively interactive system. *Q. J. R. Meteorol. Soc.*, **118**, 877-926 (1992).

Zebiak S. and Cane, M. A. Model ENSO. *Mon. Wea. Rev.*, **115**, 2262-2278 (1987)

Z. Liu, J. Kutzbach, L. Wu, Center for Climate Research, 1225 W. Dayton St., Madison, WI 53706-1695 (e-mail: zliu3@facstaff.wisc.edu, jek@facstaff.wisc.edu , lxw@ocean.meteor.wisc.edu)

(Received: January, 28,2000; Accepted: June 13, 2000.)